

# Observation of a Sharp Lambda Peak in the Third Harmonic Voltage Response of a $\text{YBa}_2\text{Cu}_3\text{O}_{7-\delta}$ Thin Film.

N. Chéenne<sup>a\*</sup>, Todor Mishonov<sup>ab</sup> and J. Indekeu<sup>a†</sup>

<sup>a</sup>Laboratorium voor Vaste-Stoffysica en Magnetisme, Katholieke Universiteit Leuven, Celestijnenlaan 200 D, B-3001 Leuven, Belgium

<sup>b</sup>Department of theoretical Physics, Sofia University St. Kliment Ohridski, 5 J. Bourchier Blvd., 1164 Sofia, Bulgaria

In this paper, we report on the sharp peak observed in the third harmonic voltage response generated by a bias sinusoidal current applied to a strip patterned in a  $\text{YBa}_2\text{Cu}_3\text{O}_{7-\delta}$  thin film, when the temperature is close to the normal-superconductor transition. The lambda-shaped temperature dependence of the third harmonic signal on the current characteristics is studied. Several physical mechanisms of third harmonic generation are examined. PACS Code/Keywords: 74.25.Fy - Third harmonic response, Non-linear voltage response, high-Tc Superconductor.

## 1. Introduction

Harmonic signals created by ac excitation have been used for a long time in the investigation of high temperature superconductors (HTSC) [1]. Particularly, a third harmonic signal is a consequence of non-linear effects and its measurement is a powerful technique to investigate, and moreover, to discriminate between the different possible origins of these non-linearities. Different techniques of third harmonic measurement exist for investigating properties of HTSC devices especially in microwave range [2]-[4], or for characterizing material properties such as thermal conductivity [5]-[8], specific heat [8], current response [9], or critical temperature [10].

As an example, measurement of the third harmonic of the ac susceptibility revealed the role of interplanar spacing on formation of flux lines and demonstrated that the irreversibility field in

$\text{Bi2212}$  is determined by surface barriers [10], [11]. This is related to vortex motion, which is one of the possible origins of the non-linear effects in electrical properties in HTSC [12]. One of the other possible roots of this non-linear behaviour is given in ref. [13], where a theoretical derivation is presented to explain non-linear effects in electrical conductivity close to the transition temperature. From this paper [13], it is expected that the measurement of the third harmonic voltage allows getting hold of superconductor constants of the BCS theory. In addition, the authors [13], [14], investigate theoretically the third harmonic voltage generation produced by the thermal response of the film to a harmonic current. Third harmonic response is definitely related to different roots of non-linear effects and should allow one to gather new information about the mechanism of HTSC non-linearity.

In the present paper, systematic measurements of the voltage response to a purely harmonic current crossing HTSC strips patterned in a  $\text{YBa}_2\text{Cu}_3\text{O}_{7-\delta}$  (YBCO) thin film were performed as a function of the temperature. First and third harmonics were recorded for the whole temperature range, from room temperature to a few Kelvin below the normal-superconductor transi-

\*Grants: This research has been supported by the Belgian DWTC, IUAP, the Flemish GOA and VIS/97/01 Programmes. T.M. is KUL Senior Fellow (F/00/038) and N.Ch. is supported by the EC TMR Network Contract nr. ERB-FMRX-CT-980171.

†Corresponding author:

phone: (+32 16) 327 127, fax.: (+32 16) 327 983,  
e-mail: joseph.indeku@fys.kuleuven.ac.be.

tion. A sharp peak was observed in the third harmonic voltage close to the critical temperature, exhibiting a lambda-shaped ( $\lambda$ -shaped) behaviour. This  $\lambda$ -shaped peak was investigated for different current amplitudes and frequencies.

Sample and measurement descriptions are given in part 2 of this paper. Complete experimental data processing and observations are presented in section 3. In section 4, mechanisms of third harmonic signal generation are briefly discussed.

## 2. Experimental setup

Measurements were all performed on two different strips designed in a YBCO thin film 180 nm thick deposited by DC sputtering on a MgO substrate, as described in [15] and [16]. The smallest is 1.59 mm long and 77  $\mu\text{m}$  wide, and the largest is 2.87 mm long and 474  $\mu\text{m}$  wide. Both were chemically etched in acid solution.

The samples were placed in a cryostat and exposed to a helium flux. The connection between the electronic equipment and the strip was made via coaxial cables in a four-points geometry (fig. 1). Strips were bias current, the latter being sinusoidally modulated with amplitude  $I_0$  and frequency  $f = \omega/2\pi$ . The rms current value  $I_0/\sqrt{2}$  was monitored during the whole experiment by measuring the voltage across the load resistance  $R_L$ , chosen large enough to have negligible variation of the current (less than 10 %). Using a digital lock-in amplifier (model SR830 from Stanford Research Systems), first ( $V_{1\omega}$ ) and third ( $V_{3\omega}$ ) harmonics of the voltage developed in the sample were successively recorded simultaneously with temperature and time.

As was mentioned in previous papers [5], [14], the current has to be much smaller than a maximal value  $I_G$ :

$$I_G = \sqrt{\frac{G}{|R'|}}, \quad (1)$$

where  $R'$  is the first derivative of the electrical resistance with respect to temperature and  $G$  is the thermal boundary conductance between the strip and the substrate, which is maintained at the temperature of the helium bath.  $G$  can be

expressed through the thermal boundary conductivity  $g$ , the length  $L$  and the width  $w$  of the strip:

$$G = gLw \quad (2)$$

Calculating  $I_G$  from standard values of  $g$  (2000 W/Kcm<sup>2</sup>) and  $R'$  (1  $\Omega$ /K) in the normal state, we found the maximal current to equal 1.6 A for the narrowest strip and 5.5 A for the widest one. In our case, the maximum current used was 14 mA, far enough from the limit given by Eq. (1).

## 3. Experimental observations

### 3.1. Experimental Data processing

Before showing our results, we explain in some detail the experimental data processing. The goal of this processing is to calculate the first and the second derivatives of the resistance with respect to temperature, which we need to estimate the thermal conductance  $G$ , as described in ref. [14]. Since our cryogenic system induces strong temperature noise, temperature data were smoothed over time, using a Savitzky-Golay filter [17], which performs a local polynomial regression to determine the smoothed value for each data point. In our case, 2<sup>nd</sup> order polynomial regression was used, taking into account 25 points to the left and 25 points to the right.

The same smoothing was used to filter the electrical resistance of the strip,  $R$ . Since the frequency  $\omega$  is in the kHz range, we consider the superconducting strip as a pure ohmic device where inductive and capacitive components are negligible. The resistance is then deduced from  $V_{1\omega}$  by Ohm's law:

$$R_{1\omega} = \frac{V_{1\omega}}{I_0} \quad (3)$$

In this case, only 5 points to the left and 5 points to the right were taken into account to perform the local regression, to avoid any big distortion close to the superconducting transition. Exactly the same procedure was applied for smoothing the third harmonic voltage.

Thus, sets of time-dependent smoothed-data were obtained and used to calculate the first and

second derivatives of the temperature ( $\dot{T}$ ,  $\ddot{T}$ ) and resistance ( $\dot{R}$ ,  $\ddot{R}$ ) with respect to time  $t$ , differentiating using Savitzky-Golay smoothing. For this step, the local smoothing was performed on the smoothed-data sets. The local regression taking into account 21 points for the temperature set and 11 points for the resistance set, allowed to deduce the first and the second derivatives for each data point. Thus, it was straightforward to determine for each point in time, the values of the first and second derivatives of the resistance with respect to temperature  $T$ :

$$R'(T) = \frac{\dot{R}}{\dot{T}}, \quad R''(T) = \frac{\ddot{R}\dot{T} - \dot{R}\ddot{T}}{(\dot{T})^3}, \quad (4)$$

All the steps of the experimental data processing are gathered in figures 2 and 3, presenting, respectively, the temperature, the resistance and their respective derivatives obtained for the narrowest strip excited by a current of 4 mA rms. The temperature was shifted by a few Kelvin during the measurements due to the poor thermal conductivity of the sample holder on which our temperature diode and sample were glued; we then shifted all temperature data sets by 4 K in order to have a reasonable  $T_c$  of 90 K for our YBCO sample.

Figure 4 and 5 give the resistance and its first and second derivatives with respect to smoothed temperature, deduced from time-dependent data set shown in figures 2 and 3, with use of eq. 4. These results were used to calculate the thermal conductance  $G$  between the strip and the heat sink, as described in [14] and to evaluate the contribution of the thermal effect in the peak observed in the third harmonic voltage  $V_{3\omega}$ , which will be described in the next section.

### 3.2. Lambda shape of the 3<sup>rd</sup> harmonic voltage $V_{3\omega}$

Figure 6 gives the third harmonic response of the narrowest strip to the current excitation with amplitude  $I_0$  equal to 5.65 mA and a modulation frequency of 1024 Hz. The behaviour of the shape and the amplitude of the peak with respect to current characteristics has been explored.

Figure 7a presents the third harmonic response

obtained for different current amplitudes, the latter varying between 0.1 mA and 4 mA rms. The first observation is that the higher is the current amplitude, the higher is the voltage peak, the width at mean height increasing much more slowly. A ratio of more than 300 between the third-harmonic peak signals is obtained for the highest and the lowest current (fig. 7a). Figure 7b presents the third harmonic amplitude, divided by the current amplitude to the power 3/2. It gives some indications about the relation between the voltage peak amplitude and the current value close to the critical temperature. In fig. 7b, the maximum ratio between peak amplitudes is only 1.5 ( $\ll 300$ ), giving a strong argument to expect a proportionality between the third harmonic amplitude and the current to the power 3/2 close to the critical temperature.

The dependence of the peak on the current frequency was study at fixed amplitude current ( $I_0 = 1.41$  mA). No differences in the peak were observed for frequencies ranging from 114 Hz to 20.6 kHz.

## 4. Discussion and conclusion

Let us discuss in brief some mechanisms for the generation of harmonics for different temperatures and physical situations. At very low temperature, in the vortex pinning regime or in a vortex-free situation, modulation of the superconducting order parameter creates dissipation and harmonic generation [18] [19]; the non-linearity is created by the current dependence of the superfluid density which can be easily described within the Ginzburg-Landau model [20]. Non-linear response of the vortex state [12] can also create higher harmonics. However, the complexity of the pinning mechanisms and the generation of magnetic field by the applied current makes it very difficult to develop a detailed theory for the  $\lambda$ -shaped maximum. For example, small superconducting grains in a diamond anvil [10], [11], or scanning of the surface of a thin film by a terminated co-axial cable [2] require the solution of different electrodynamics problems. In our paper, we used a narrow strip and the vortices are created near the edges of the sample by the ap-

plied current. The generation of the vortices can be significantly decreased if a Corbino-geometry is used; it is necessary that a superconducting film terminates a coaxial cable.

For temperatures slightly above the critical one, there is significant fluctuation conductivity. Usual ohmic conductivity of normal carriers is perfectly linear but fluctuation conductivity is not and can create observable part of the harmonic generation [13].

For higher temperatures, temperature oscillations can create harmonics in the voltage response [5], [6], [14], [21]. Analogously to temperature oscillations well above  $T_c$ , a quite universal mechanism for 3<sup>rd</sup> harmonic generation at microwave frequencies exists for the superconducting state below  $T_c$ . The density of superfluid particles depends on the applied current and finally the kinetic inductance of the superconducting sample depends on the current  $I = I_0 \cos(\omega t)$

$$L(I) \approx L_0 + L_1 I^2. \quad (5)$$

$L_0$  gives the linear contribution to the kinetic inductance and  $L_1$  the non-linear one (see ref. [18], [19]). Then, the general formula for the voltage response given by

$$V(t) = L(I) \frac{dI}{dt} \quad (6)$$

allows to calculate the third harmonic response [18], [19]:

$$V_{3\omega} = -\frac{L_1 \omega I_0^3}{4} \sin(3\omega t) \quad (7)$$

It appears in this formula that the third harmonic response increases linearly with the frequency. This explains that it is typically observed in the microwave range devices. In our range of frequencies (up to 20kHz), this response is not expected to be observable.

The main quantitative property of the third harmonic response is the sharp  $\lambda$ -peak close to the critical temperature. Detailed investigation of the dependence of the height and width of this peak on the current and geometry of the strip will be the theme of further research. These measurements should be helpful to discriminate the different contributions to the third harmonic

response, close to the critical temperature, i.e. the thermal oscillation part and the non-linear conductivity part. The same data procedure will be employed to analyse our future experimental data.

In conclusion, the investigation of the  $\lambda$ -peak of the third harmonic response is a good qualitative method for the detection of the superconducting phase transition. Because of the simplicity of the measurement, it can become a standard method in the materials science of superconductors.

Detailed investigation of the third harmonic response provides a reliable method for the investigation of superconductor thermal properties like thermal conductivity, thermal boundary resistance and heat capacity. Moreover, if the thermal effects are carefully subtracted, the investigation of the third harmonic signal will provide the opportunity to extract the relaxation time of the superconducting order parameter from the isothermal electric non-linearity. If Corbino geometry does not create significant heating of the sample, this can be expected to be the best experimental setup for the observation of Cooper-pair depairing non-linearity.

### Acknowledgments

Special thanks goes to Dr. Patrick Wagner [15] who provided us with a high-quality YBCO thin film. Also we would like to express our gratitude to Dr. Johan Vanacken for assistance with the experiments. T.M. would like to thank V. Mishonova for bringing ref. [31] to his attention, where the equations for thermal oscillations in superconductor microbolometers were derived for the first time.

### REFERENCES

1. L. Ji, R.H. Sohn, G.C. Spalding, C.J. Lobb and M. Tinkham, "Critical-state model for harmonic generation in high-temperature superconductors", Phys. Rev. B **40**(16) (1989) 10936-10945; and references [2]-[6] therein.
2. E.E. Pestov, Y.N. Nozdrin and V.V. Kurin, "Third-order local nonlinear microwave response of YBa<sub>2</sub>Cu<sub>3</sub>O<sub>7</sub> and Nb thin films",

- ASC2000, Virginia Beach, Virginia, 17-22 Sept. 2000 - Published in IEEE Trans. on Appl. Supercond. **11** (2001) 131-134; E.E. Pestov, Y.N. Nozdrin and V.V. Kurin, "A new method for a local study of nonlinear microwave properties of superconductors", cond-mat/0005501. In this paper are discussed some mechanisms of surface resistance nonlinearity. In Ref. 2 of this paper, a correlation was found between the depinning current density and the nonlinear microwave response.
3. J.C. Booth, J.A. Beall, R.H. Ono, F.J.B. Stork, D.A. Rudman and L.R. Vale, "Third order harmonic generation in high temperature superconducting coplanar wave guides at microwave frequencies", IEEE Trans. Appl. Supercond. **5** (1995) 2652-2655.
  4. H. Shimakage, J.C. Booth, L.R. Vale and R.H. Ono, "Third harmonics generation from YBaCuO Bicrystal Josephson junctions in coplanar waveguides", Supercond. Science and Techn. **12** (1999) 830-832.
  5. D. Robbes, N. Chéenne, J.F. Hamet and J.P. Rice, "Thermal boundary resistance of a YBCO/STO multilayer strip", IEEE Trans. Appl. Supercond. **9** (1999) 3874-3877; In Eq.(1) of this paper,  $I_0^3$  is misprinted as  $I_0^2$ , cf. next ref. [6].
  6. N. Chéenne, "Synthèse de films minces de type superréseau pour la réalisation et l'étude de micro-bolomètres. Rôle des interfaces sur la transmission des phonons" ("The study and design of multilayered microbolometers, and the role of the interfaces on the reflection of phonons"), Ph. D. Thesis, University of Caen, France (Dec. 2000) p. 127, Eq. (III-46) (in French, unpublished); a copy is available upon request to ncheenne@greyc.ismra.fr.
  7. T. Borca-Tasciuc, A.R. Kumar and G. Chen, "Data reduction in 3w method for thin-film thermal conductivity determination", Rev. Sci. Instrum. **72** (2001) 2139-2147.
  8. L. Lu, W. Yi and D.L. Zhang, "3w method for specific heat and thermal conductivity measurements", Rev. Sci. Instrum. **72** (2001) 2996-3003; and ref. therein, especially the historical paper for thermal information extracted from ac heating (O.M. Corbino, Phys. Z. **11** (1910) 413.)
  9. T. Dahm and D.J. Scalapino, "Nonlinear current response of a d-wave superfluid", Phys. Rev. B **60** (1999) 13125-13130.
  10. M.P. Raphael, M.E. Reeves and E.F. Skelton, "Nonlinear response of type II superconductors: a new method of measuring the pressure dependence of the transition temperature,  $T_c(P)$ ", Rev. Sci. Instrum. **69** (1998) 1451-1455.
  11. M.P. Raphael, M.E. Reeves, E.F. Skelton and C. Kendziora, "Pressure dependence of the irreversibility line in  $\text{Bi}_2\text{Sr}_2\text{CaCu}_2\text{O}_{8+\delta}$ : Role of anisotropy in flux-line formation", Phys. Rev. Lett. **84** (2000) 1587-1590.
  12. R. Mallozi, J. Orenstein, J.N. Eckstein, and I. Bozovic, "High-Frequency Electrodynamics of  $\text{Bi}_2\text{Sr}_2\text{CaCu}_2\text{O}_{8+\delta}$ : Nonlinear Response in the Vortex State", Phys. Rev. Letters **81** (1998) 1485-1488.
  13. T. Mishonov, A. Posazhennikova and J. Indekeu, "Fluctuation conductivity in superconductors in strong electric fields", cond-mat/0106168, submitted to Phys. Rev. B (unpublished).
  14. T. Mishonov, N. Chéenne, D. Robbes and J. Indekeu, "Generation of 3rd and 5th harmonics in a thin superconducting film by temperature oscillations and isothermal nonlinear current response", submitted for publication to Eur. J. Phys. (unpublished).
  15. P. Wagner, F. Hilmer, U. Frey, H. Adrian, T. Steinborn, L. Ranno, A. Elschner, I. Heyvaert and Y. Bruynseraede, "Preparation and structural characterization of thin epitaxial  $\text{Bi}_2\text{Sr}_2\text{CaCu}_2\text{O}_{8+\delta}$  films with  $T_c$  in the 90K range", Physica C **215** (1993) 123-131.
  16. B. Wuyts, Z.X. Gao, S. Libbrecht, M. Maenhoudt, E. Osquiguil and Y. Bruynseraede, "Growth of particle-free  $\text{YBa}_2\text{Cu}_3\text{O}_{7-\delta}$  films by off-axis sputtering", Physica C **203** (1992) 235-239.
  17. W.H. Press, S.A. Teukolsky, B.P. Flannery and W.T. Vetterling, "Numerical Recipes in C", Cambridge University Press, New York, USA, 2nd Edition (1992), Fig. 14.8.2, p. 654.
  18. J.C. Booth, J.A. Beall, D.A. Rudman, L.R.

- Vale and R.H. Ono, "Geometry dependence of nonlinear effects in High Temperature Superconducting transmission lines at microwave frequencies", J. Appl. Phys. **86** (1999) 1020-1027.
19. J.C. Booth, L.R. Vale, R.H. Ono and J.H. Claassen, "Power-dependent impedance of High Temperature Superconductor thin films: Relation to harmonic generation", J. Supercond.: Incorp. Novel Magnetism **14** (2001) 65-72.
  20. E.S. Borovitskaya, V.M. Leviev and G.I. Genkin, "Nonlinear microwave response of YBaCuO superconducting film", JEPT **83** (1996) 597.
  21. A.A. Zharov, A.L. Korotkov, A.N. Reznik, Supercond. **5** (1992) 413;  
 A.A. Zharov, A.L. Korotkov, A.N. Reznik, "Electromagnetic power limiting at S-N transition in a thin superconducting film", Supercond. Sci. Technol. **5** (1992) 104-106; and ref. [6] therein: Richards P.L. et al., Ext. Abstr. 3rd Int. Superconductive Electronics Conf. 25-27 June 1991, University of Strathclyde, Glasgow, Scotland, p. 15;  
 A.L. Korotkov, A.N. Reznik and A.A. Zharov, "Thermo-electric oscillations in HTSC film structures: estimation of thermal parameters", Supercond. Sci. Technol. **9** (5) (1996) 353-357.

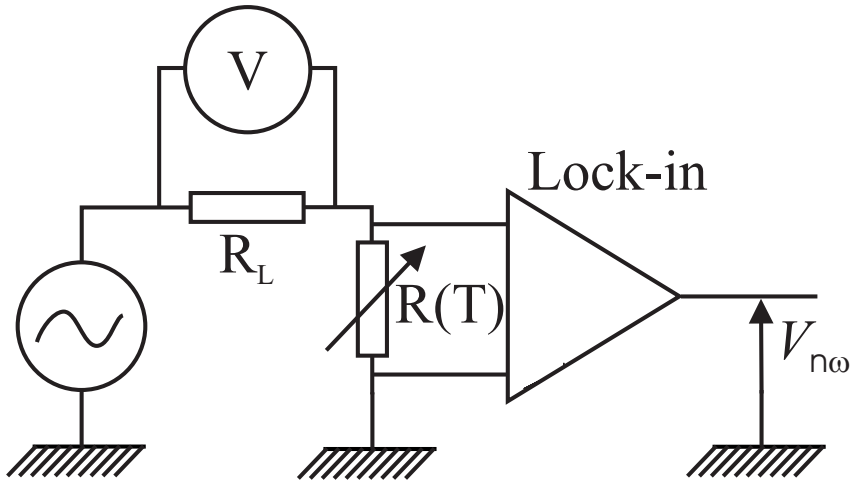


Figure 1. Scheme of electrical measurements. The current in the superconductor sample (symbolized by its temperature-dependent resistance  $R(T)$ ) is governed by the voltage generator and the load resistance  $R_L$ . The voltmeter across  $R_L$  allows to monitor the current in the sample. The rms voltage harmonic response ( $V_{nw} \div \sqrt{2}$ ,  $n = 1, 3$ ) across the sample is measured by a lock-in amplifier and recorded as a function of temperature.

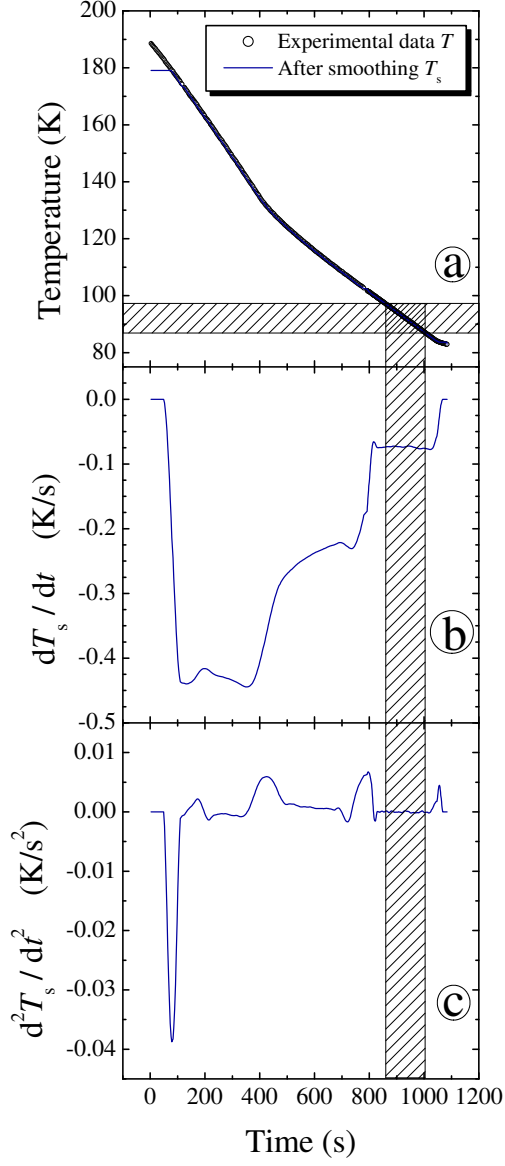


Figure 2. Recording of temperature  $T$  vs time (a), and first (b) and second (c) derivatives of its smoothed values  $T_s$ .

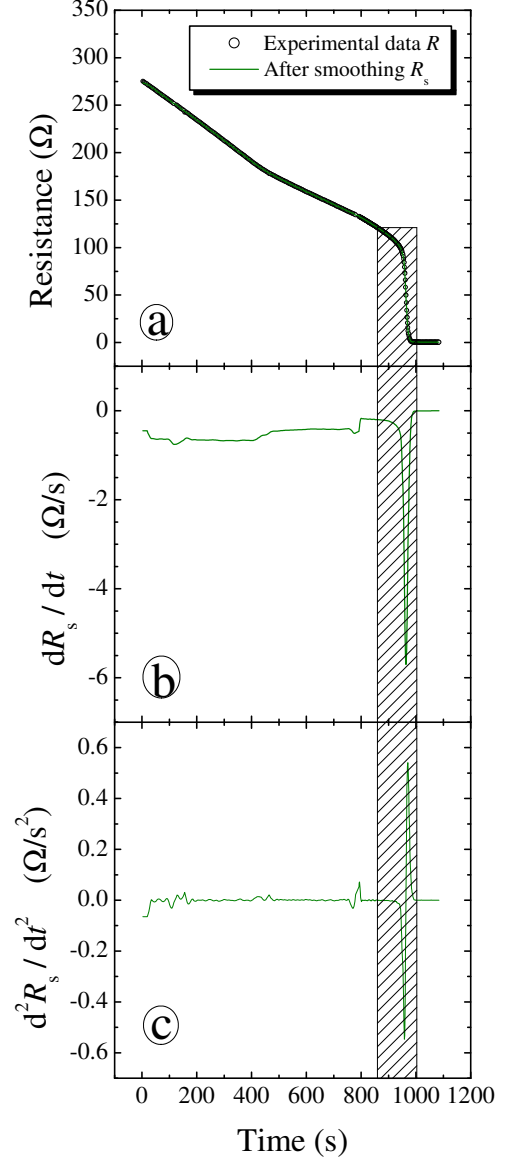


Figure 3. Recording of resistance  $R$  vs time (a), and first (b) and second (c) derivatives of its smoothed values  $R_s$ .



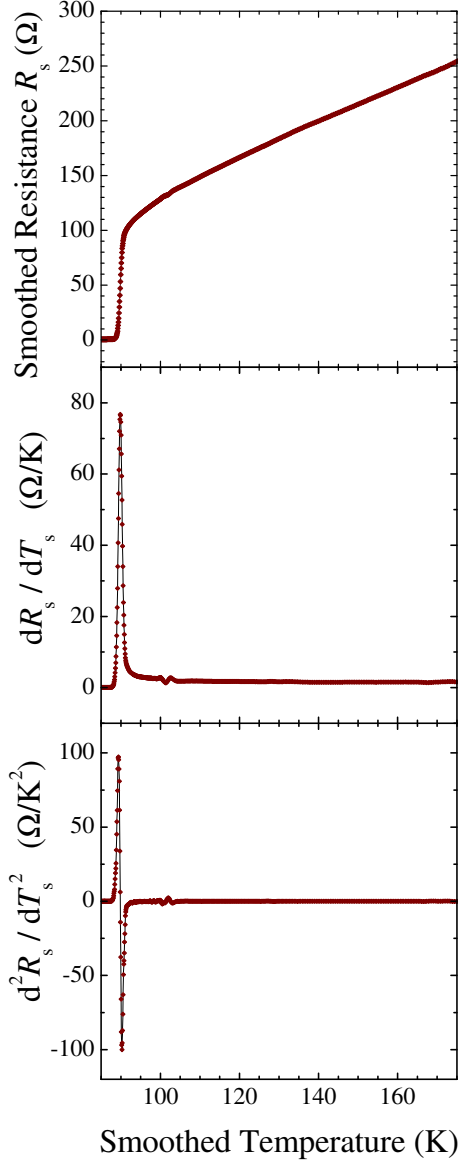


Figure 4. The resistance and its first and second derivatives with respect to temperature deduced from eq. 4 and data sets extracted from figures 2 and 3.

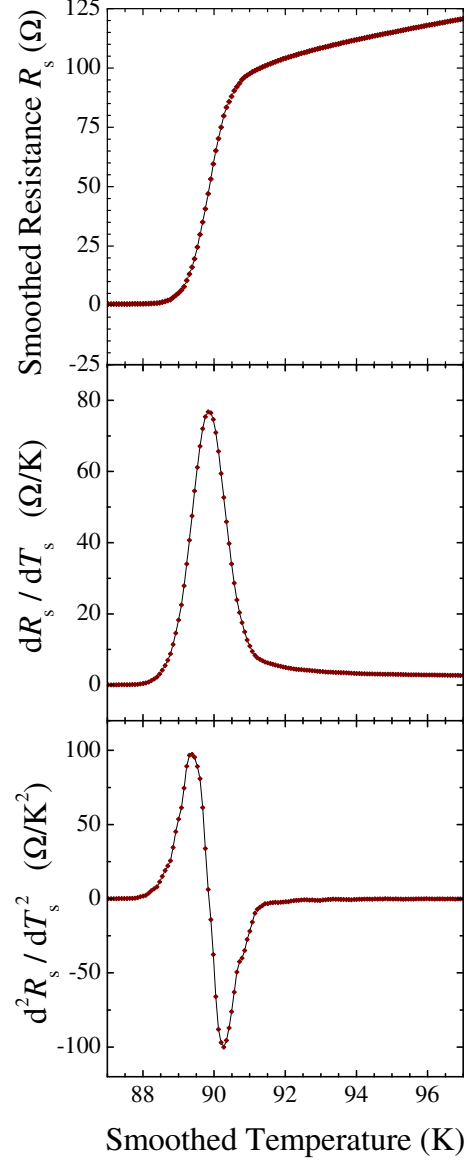


Figure 5. The resistance and first and second derivative with respect to temperature, on the temperature range indicated by the hatched areas on figures 2 and 3.

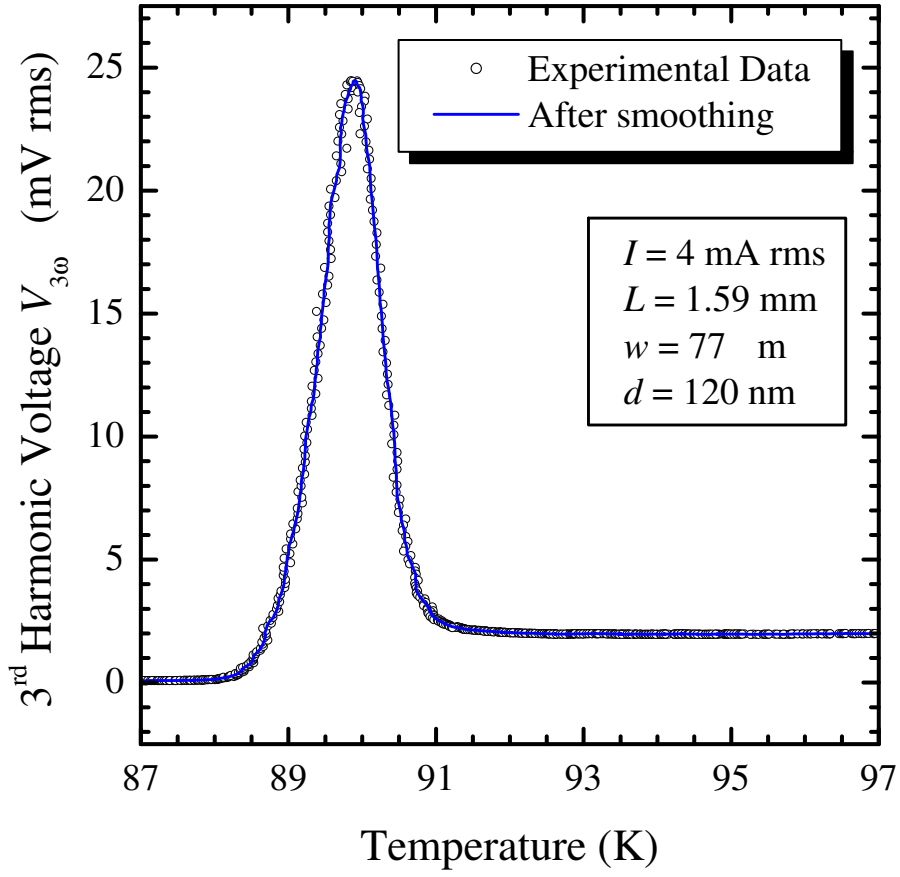


Figure 6.  $\lambda$ -shaped temperature dependence of the third harmonic voltage  $V_{3\omega}$ .

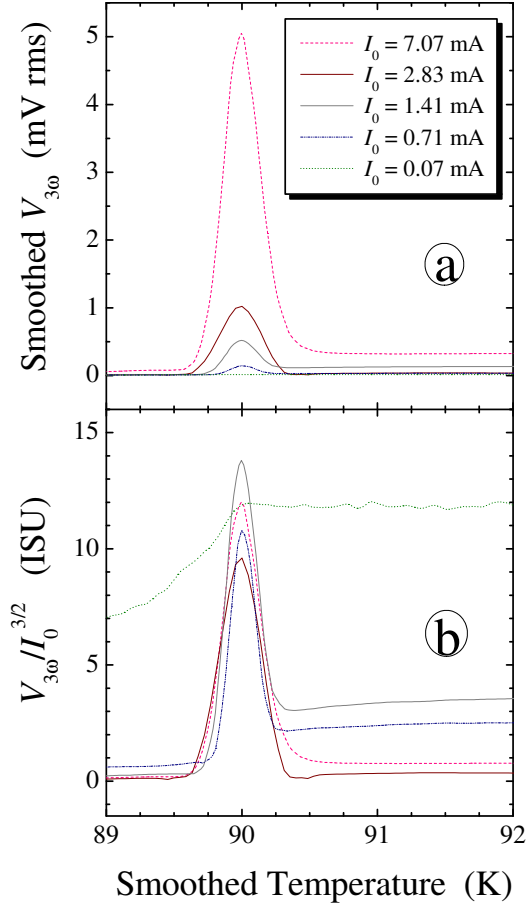


Figure 7. Dependence of the third harmonic signal on temperature for different current amplitudes. In figure 7a, the increase of the peak amplitude with current amplitude  $I_0$  is demonstrated. Figure 7b shows the proportionality between  $V_{3\omega}$  and  $I_0^{3/2}$  close to the critical temperature.